ACTA ASTRONOMICA
Vol. **53** (2003) pp. 93–116

The Optical Gravitational Lensing Experiment. Catalog of RR Lyr Stars in the Large Magellanic Cloud*

by

I. Soszyński[1], A. Udalski[1], M. Szymański[1],
M. Kubiak[1], G. Pietrzyński[1,2], P. Woźniak[3],
K. Żebruń[1], O. Szewczyk[1] and Ł. Wyrzykowski[1]

[1] Warsaw University Observatory, Al. Ujazdowskie 4, 00-478 Warszawa, Poland
e-mail: (soszynsk,udalski,msz,mk,pietrzyn,zebrun,szewczyk,wyrzykow)@astrouw.edu.pl
[2] Universidad de Concepción, Departamento de Fisica, Casilla 160–C, Concepción, Chile
[3] Los Alamos National Laboratory, MS-D436, Los Alamos, NM 87545 USA
e-mail: wozniak@lanl.gov

Received May 30, 2003

ABSTRACT

We present the catalog of RR Lyr stars discovered in a 4.5 square degrees area in the central parts of the Large Magellanic Cloud (LMC). Presented sample contains 7612 objects, including 5455 fundamental mode pulsators (RRab), 1655 first-overtone (RRc), 272 second-overtone (RRe) and 230 double-mode RR Lyr stars (RRd). Additionally we attach a list of several dozen other short-period pulsating variables. The catalog data include astrometry, periods, *BVI* photometry, amplitudes, and parameters of the Fourier decomposition of the *I*-band light curve of each object.

We present density map of RR Lyr stars in the observed fields which shows that the variables are strongly concentrated toward the LMC center. The modal values of the period distribution for RRab, RRc and RRe stars are 0.573, 0.339 and 0.276 days, respectively. The period–luminosity diagrams for *BVI* magnitudes and for extinction insensitive index W_I are constructed. We provide the $\log P{-}I$, $\log P{-}V$ and $\log P{-}W_I$ relations for RRab, RRc and RRe stars. The mean observed *V*-band magnitudes of RR Lyr stars in the LMC are 19.36 mag and 19.31 mag for ab and c types, respectively, while the extinction free values are 18.91 mag and 18.89 mag.

We found a large number of RR Lyr stars pulsating in two modes closely spaced in the power spectrum. These stars are believed to exhibit non-radial pulsating modes. We discovered three stars which simultaneously reveal RR Lyr-type and eclipsing-type variability. If any of these objects were an eclipsing binary system containing RR Lyr star, then for the first time the direct determination of the mass of RR Lyr variable would be possible.

We provide a list of six LMC star clusters which contain RR Lyr stars. The richest cluster, NGC 1835, hosts 84 RR Lyr variables. The period distribution of these stars suggests that NGC 1835 shares features of Oosterhoff type I and type II groups.

All presented data, including individual *BVI* observations and finding charts are available from the OGLE INTERNET archive.

Key words: *Stars: variables: RR Lyr – Magellanic Clouds – Catalogs*

*Based on observations obtained with the 1.3 m Warsaw telescope at the Las Campanas Observatory of the Carnegie Institution of Washington.

1. Introduction

RR Lyr stars have been recognized as excellent tracers of the oldest stellar populations, as well as distance indicators of the Galactic and extragalactic stellar systems. These stars are among the most prominent members of Population II objects, easy to identify due to their characteristic pulsation periods, shape of the light curves, luminosities and colors.

The Large Magellanic Cloud (LMC), as the nearest non-dwarf galaxy, plays a key role in studying a wide variety of astrophysical problems, because one can assume that the stars in the LMC are located, in the first approximation, at the same, relatively small distance. Since the population of RR Lyr variables in the LMC is extremely rich, many important problems, including the distance scale, structural and chemical evolution of the Local Group galaxies, features and properties of the old-age stars may be studied with these stars.

The first major survey for RR Lyr stars in the LMC was performed by Thackeray and collaborators (Thackeray and Wesselink 1953). They found variables in the clusters NGC 1466 and NGC 1878. Surveys for field RR Lyr stars in the Magellanic Clouds were initiated by Graham (1977). Sixty eight RR Lyr variables were discovered in a $1^\circ \times 1\overset{\circ}{.}3$ field around the globular cluster NGC 1783. The subsequent surveys for the LMC RR Lyr stars (Kinman *et al.* 1976, Nemec *et al.* 1985, Walker 1992, Hazen and Nemec 1992) increased the number of known RR Lyr variables mainly in the outer fields of the LMC where density of stars is lower than in the central parts.

The crucial moment in studies of RR Lyr stars from the LMC was announcement of discovery of about 7900 such stars in 22 fields in the bar region of the LMC by the MACHO microlensing group (Alcock *et al.* 1996). In following papers the MACHO team presented discovery of 181 double-mode RR Lyr variables (Alcock *et al.* 1997, 2000), and detected non-radial pulsations in the first-overtone RR Lyr stars (Alcock *et al.* 2000). Small scale survey for RR Lyr (about 100 objects) was also presented by Clementini *et al.* (2003).

The Optical Gravitational Lensing Experiment (OGLE; Udalski, Kubiak and Szymański 1997) is the long term large microlensing survey started in the early 1990s. The LMC was included to the list of observed targets of the OGLE survey at the beginning of the second phase of the project (OGLE-II), in January 1997. The galaxy was regularly monitored to the end of the OGLE-II phase, *i.e.*, to November 2000. The LMC is also one of the main targets of the third phase of the project (OGLE-III), which started in June 2001.

The OGLE-II survey substantially increased the number of known variable stars in both Magellanic Clouds. In the previous papers we presented the catalogs of eclipsing binary stars in the Magellanic Clouds (Udalski *et al.* 1998b, Wyrzykowski *et al.* 2003), catalogs of Cepheids in the Magellanic Clouds (Udalski *et al.* 1999ab), catalog of RR Lyr stars in the SMC (Soszyński *et al.* 2002, hereafter Paper I) and general catalog of variable stars detected in the Magellanic Clouds (Żebruń *et al.*

2001). In addition, *BVI* maps of the LMC and SMC were released providing precise photometry and astrometry of about 7 and 2 million stars from these galaxies, respectively (Udalski *et al.* 1998a, 2000).

In this paper we present the catalog of 7612 RR Lyr stars and several other pulsating objects, likely δ Sct stars, detected in the OGLE-II fields in the LMC. The stars were selected from the reprocessed OGLE-II photometry based on the Difference Image Analysis (DIA) technique. We provide all basic observational parameters of detected stars and present statistics of the most important parameters. The photometry and finding charts of all detected objects are available to the astronomical community from the OGLE INTERNET archive.

2. Observations and Data Reductions

All observations presented in this paper were carried out during the second phase of the OGLE microlensing search with the 1.3-m Warsaw telescope at Las Campanas Observatory, Chile. The observatory is operated by the Carnegie Institution of Washington. The telescope was equipped with the "first generation" camera with a SITe 2048×2048 CCD detector working in drift-scan mode. The pixel size was 24 μm giving the 0.417 arcsec/pixel scale. Observations of the LMC were performed in the "slow" reading mode of the CCD detector with the gain 3.8 e^-/ADU and readout noise of about 5.4 e^-. Details of the instrumentation setup can be found in Udalski, Kubiak and Szymański (1997).

Observations presented in this paper were conducted between January 6, 1997 and November 26, 2000. Eleven driftscan fields (LMC_SC1–LMC_SC10 and LMC_SC12), each covering $14\farcm2 \times 57'$ on the sky, were observed since January 1997. Additional ten fields (LMC_SC11 and LMC_SC13–LMC_SC21), added in October 1997, increased the total observed area of the LMC to about 4.5 square degrees. Photometry was obtained with the BVI filters, closely resembling the standard system. Due to microlensing search observing strategy the majority of frames were taken in the I photometric band (about 260–520 epochs depending on the field). The remaining images were collected through the *V*-band (typically about 30–70 epochs) and *B*-band (about 30 epochs) filters. The effective exposure time lasted 125, 174 and 237 seconds for the I, V and *B*-band, respectively. The median seeing was about $1\farcs3$ for our dataset.

The analysis of the dataset was performed according to the procedures described in Paper I. The *I*-band photometry was obtained using Difference Image Analysis (DIA) – image subtraction algorithm developed by Alard and Lupton (1998) and Alard (2000), and implemented by Woźniak (2000). The DIA photometry pipeline was rerun on the complete set of OGLE-II images and the code included several modifications compared to the first application of the method (Żebruń *et al.* 2001). We found that the detection efficiency of faint variable objects (in particular RR Lyr stars) in the Żebruń *et al.* (2001) catalog was relatively poor.

The details of the DIA analysis and calibration of photometry may be found in Woźniak (2000) and Żebruń, Soszyński and Woźniak (2001). The DOPHOT photometry package (Schechter, Saha and Mateo 1993) was used to determine V and B-band magnitudes of the stars. For more details about data reduction and transformation procedures the reader is referred to Udalski *et al.* (2000).

Equatorial coordinates of all stars were calculated in the identical manner as described in Udalski *et al.* (2000). The internal accuracy of the determined equatorial coordinates, as measured in the overlapping regions of neighboring fields, is about $0\farcs15$–$0\farcs20$ with possible systematic errors of the DSS coordinate system up to $0\farcs7$.

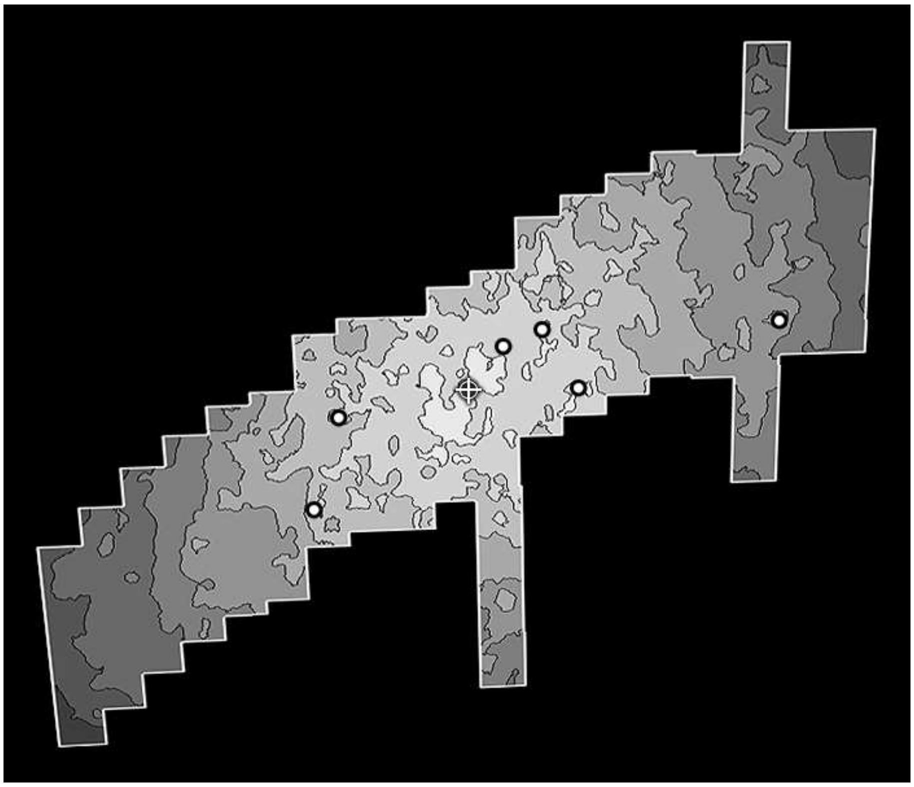

Fig. 1. Density map of RR Lyr stars in the LMC. White circles indicate positions of star clusters where RR Lyr stars were found. The cross marks probable center of the LMC.

Fig. 1 presents density map of the RR Lyr variables from the LMC. One can notice that, contrary to the RR Lyr stars in the SMC (Paper I), RR Lyr variables in the LMC are strongly concentrated toward the galaxy center. The highest density region and approximately the center of the presented distribution has the equatorial coordinates RA=$5^{\mathrm{h}}22\fm9$ DEC=$-69^{\circ}39'$. It is possible that this is the center of the LMC.

3. Interstellar Reddening

The reddening map of the OGLE-II fields in the LMC was derived by Udalski *et al.* (1999a). Since the reddening toward the LMC is clumpy and variable, the mean reddening values were determined in 84 lines-of-sight – four per each OGLE-II field. Udalski *et al.* (1999a) used red clump stars for mapping the fluctuations of the mean reddening in the LMC, taking their mean *I*-band magnitude as the reference brightness. Differences of the observed mean *I*-band magnitudes were assumed as differences of the mean A_I extinction, and then converted to differences of $E(B-V)$. The zero points of the reddening map were derived based on previous determinations of reddening around clusters NGC 1850, NGC 1835, and in the field of the eclipsing variable star HV2274.

Table 1

$E(B-V)$ reddening in the LMC fields

Field	Subfield 1 $E(B-V)$	Subfield 2 $E(B-V)$	Subfield 3 $E(B-V)$	Subfield 4 $E(B-V)$
LMC_SC1	0.117	0.152	0.147	0.163
LMC_SC2	0.121	0.121	0.150	0.131
LMC_SC3	0.134	0.120	0.123	0.117
LMC_SC4	0.130	0.120	0.105	0.118
LMC_SC5	0.130	0.115	0.108	0.133
LMC_SC6	0.138	0.125	0.107	0.123
LMC_SC7	0.143	0.138	0.142	0.146
LMC_SC8	0.131	0.133	0.136	0.142
LMC_SC9	0.143	0.165	0.156	0.149
LMC_SC10	0.156	0.147	0.146	0.132
LMC_SC11	0.147	0.154	0.150	0.152
LMC_SC12	0.152	0.146	0.127	0.139
LMC_SC13	0.154	0.129	0.135	0.130
LMC_SC14	0.124	0.142	0.138	0.127
LMC_SC15	0.145	0.125	0.147	0.126
LMC_SC16	0.135	0.148	0.185	0.181
LMC_SC17	0.171	0.193	0.175	0.201
LMC_SC18	0.182	0.178	0.173	0.170
LMC_SC19	0.153	0.153	0.187	0.167
LMC_SC20	0.132	0.137	0.142	0.163
LMC_SC21	0.133	0.152	0.145	0.146

The final $E(B-V)$ reddening in our LMC fields is listed in Table 1. The error of the map is estimated to be ± 0.02 mag. Interstellar extinction in the *BVI* bands can be calculated using the standard extinction curve coefficients (*e.g.*, Schlegel *et al.* 1998):

$$A_B = 4.32 \cdot E(B-V), \quad A_V = 3.24 \cdot E(B-V), \quad A_I = 1.96 \cdot E(B-V)$$

4. Selection of RR Lyr Stars

The search for variable objects in the LMC fields was performed using observations in the *I*-band as they are much more numerous than in other bands. First, a preliminary search for RR Lyr variables was performed using the regular OGLE-II PSF (DoPHOT) photometry. Candidates for variable stars were selected based on comparison of the standard deviation of all individual measurements of a star with typical standard deviation for stars of similar brightness. Light curves of selected candidates were searched for periodicity using the AoV algorithm (Schwarzenberg-Czerny 1989). Light curves of all objects revealing statistically significant periodic signal were then visually inspected and divided into a few groups of variable stars.

In the second stage we checked variability of stars using their DIA photometry. We selected stars with the mean *I*-band magnitude in the range 15 mag to 20 mag, and with the standard deviation of photometry at least 0.01 mag bigger than the median value of standard deviation for stars at given brightness. Photometry of each star from this list was subject to a period-searching program FNPEAKS (Kołaczkowski 2003 – private communication). This algorithm is relatively fast what made it possible to test about 2 million stars. The output from FNPEAKS contains the most significant peaks from the power spectrum (we checked three most significant frequencies of all stars) with a signal-to-noise parameter characterizing each peak. Then, we performed Fourier analysis of stars with periods shorter than 1 day, and signal-to-noise higher than 3.5, *i.e.*, corresponding to the boundary between constant and variable stars. For further analysis we selected objects which occupy appropriate region in the $\log P\text{–}R_{21}$ diagram (see Section 8.4). In the final step, each object was carefully checked visually. Other type of variable stars and obvious artifacts were removed from the sample.

While the vast majority of non-pulsating variable stars were removed from the catalog in the selection process, it is possible that some of the eclipsing binary stars could remain on the list of RRc stars, especially when they have similar luminosity and colors like RR Lyr stars. It is also likely that a limited number of other type of short-period pulsators, like δ Sct stars, anomalous Cepheids, pulsating blue stragglers, etc. are hidden among our sample of RR Lyr object candidates.

5. Classification

5.1. Single-Mode RR Lyr stars

All selected variable star candidates were divided into five groups: fundamental mode RR Lyr stars (RRab), first overtone (RRc), second overtone (RRe), double mode RR Lyr stars (RRd) and other variables.

The primary criterion of classification of single-mode RR Lyr stars was their location in the $\log P\text{–}R_{21}$ diagram (see Section 8.4). When the errors of the Fourier parameter R_{21} were large and in doubtful cases we also used the $\log P$–amplitude diagram (see Section 8.3). Fundamental mode and first-overtone pulsators form well-separated groups in both diagrams, so that selection of these classes of RR Lyr stars was not difficult.

The second-overtone RR Lyr stars are thought to form a secondary peak in the period distribution of overtone RR Lyr variables. Such a peak, around $P = 0.281$ days, was first discovered and interpreted by Alcock *et al.* (1996). Studying $\log P$–R_{21} and $\log P$–amplitude diagrams we noticed that stars with period smaller than about 0.3 days can be divided into two groups: sinusoidal and low amplitude pulsators and more asymmetric higher amplitude RR Lyr stars. Similarly to Clement and Rowe (2000), who studied OGLE photometry of RR Lyr stars from the globular cluster ω Cen, we assumed that the first group is formed by RRe, *i.e.*, second-overtone stars.

However, one should remember that other interpretations of these short-period low-amplitude stars are also possible. For example, models of Bono *et al.* (1997) indicate that period–amplitude sequence of RRc stars has a characteristic "bell" shape, *i.e.*, the first-overtone pulsators with shortest periods should have lower amplitudes. Kovács (1998) presented aguments that this short-period class of RR Lyr variables are first-overtone pulsators. He used pulsation models and evolutionary calculations to show that the second-overtone oscilations with a period as long as 0.28 days are not possible. Moreover, Stellingwerf, Gautschy and Dickens (1987) theoretically predicted that the second-overtone RR Lyr stars should have sharper peak at maximum of light than first-overtone pulsators. We do not find such effect in our observational data – light curves of our RRe candidates are more symmetrical than light curves of RRc stars at the same periods.

In contrast to the fundamental mode and first-overtone RR Lyr stars, the observational parameters of RRc and RRe variables overlap, thus it is difficult to make definitive classification. We stress that our division into first- and second-overtone RR Lyr stars has only statistical sense and in individual cases might be wrong.

5.2. Multi-Mode RR Lyr stars

Double-mode RR Lyr stars (RRd) are relatively easy to detect, because of their well defined range of the period ratio. First, the preliminary search for RRd stars was carried out using the output of FNPEAKS. We selected for visual inspection objects for which the ratio of the two of three highest peaks in the power spectrum was close to 0.745. The second search for double-mode RR Lyr stars was performed by fitting a fourth order Fourier series to each light curve from our sample and subtracting fitted function from the observational data. Then, the residuals were searched for other periodic signals and, if detected, such a candidate was marked for visual inspection.

During the process of selection of double-mode RR-Lyr variables we discovered numerous class of multi-periodic stars which exhibit two frequencies, very closely spaced. We found that such a phenomenon occurs in about 15% of RRab, 6% of RRc and 23% of RRe stars, although one should remember that we performed only preliminary frequency analysis. The range of period ratios of the secondary and primary periodicities depends on the RR Lyr type: for RRab stars it is usually from 0.98 to 1.03, for RRc and RRe stars the period ratio ranges from 0.95 to 1.07, although smaller and larger ratios also sometimes occur.

This class of multi-periodic RR Lyr variables was described by Olech *et al.* (1999), who found such stars in the globular clusters M5 and M55. They argued that such a behavior is caused by the presence of non-radial oscillations in those stars. Alcock *et al.* (2000) performed frequency analysis of the variables from the LMC classified previously as RRc stars and divided multi-periodic pulsators into nine groups according to their frequency spectra. High period ratios in RR Lyr stars were also detected in the OGLE Galactic bulge RR Lyr sample (Moskalik 2000) and in RR Lyr stars from the SMC (Paper I). Theoretical models of these stars were proposed by Van Hoolst, Dziembowski and Kawaler (1998), Dziembowski and Cassisi (1999), Nowakowski and Dziembowski (2001). An extensive and careful frequency analysis of objects from our catalog should allow to detect a large variety of multi-periodic and non-stationary RR Lyr stars.

We also found a few double-mode variables with periods and period ratios outside the region occupied by "classical" RRd stars. Probably four stars with the period ratio of about 0.76 and longer periods between 0.2 and 0.4 days are double-mode δ Sct stars. Two similar stars were detected in the SMC (Paper I). Additional four stars are double-mode pulsators with period ratios from 0.8028 to 0.8062 and the longer dominant periods between 0.3 and 0.4 days. Three of these stars were discovered by MACHO (Alcock *et al.* 2000). Such ratio of periods is theoretically predicted as an indicator of RR Lyr variables pulsating in the first and second overtone. Because these objects are about 1 mag brighter than typical RR Lyr stars, and their light curves are different than light curves of RR Lyr stars, we suggest that these are other type of variable stars, perhaps short period double-mode Cepheids. Further observations and studies of these objects would be necessary to confirm their status.

Finally, we detected three objects exhibiting simultaneously the RR Lyr and eclipsing binary star type of variability. Their light curves are presented in Fig. 2. In the first two columns original light curves folded with pulsation and eclipsing periods are presented. The third and fourth columns show the light curve of RR Lyr and eclipsing star after subtracting the other variability.

The stars can be either optical blends of a RR Lyr star with physically unrelated eclipsing system unresolved within the seeing disk or eclipsing systems containing RR Lyr object as one of the components. The latter case would be extremely interesting and of great importance as the photometric and spectroscopic follow-up observations should allow for the first time to directly determine the mass and radius of RR Lyr star.

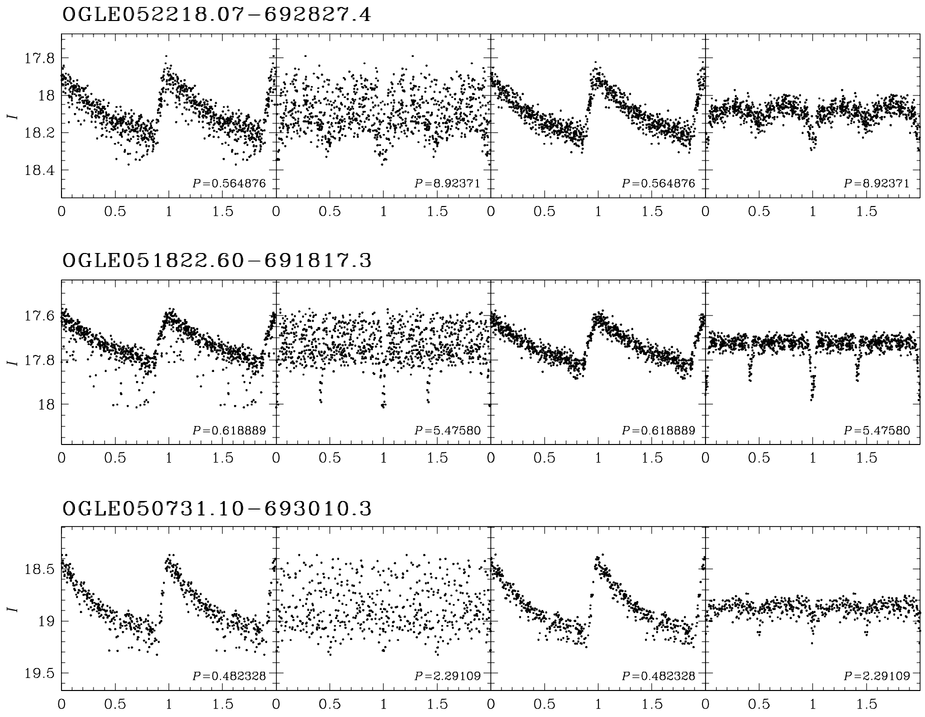

Fig. 2. Light curves of three RR Lyr stars revealing also eclipsing variability. In the first two columns the original photometric data folded with the RR Lyr period and eclipsing period are presented. In the third and the fourth columns RR Lyr and eclipsing light curves after subtracting the other component are shown.

Our preliminary analysis suggests that OGLE050731.10–693010.3 is probably an optical blend. The eclipsing period is too short for the system to be physically related: the typical RR Lyr star would be larger than the corresponding Roche lobe. In the case of OGLE051822.60–691817.3 the situation is unclear. The RR Lyr component could fit its Roche lobe but it should be close to its size. So the star should be tidally distorted. On the other hand the shape of the eclipsing light curve with flat parts between eclipses does not show any significant ellipsoidal effect. Thus OGLE052218.07–692827.4 remains the best candidate for an eclipsing system containing RR Lyr component. As all objects are within reach of accurate spectroscopy obtained with large 8-m class telescopes, radial velocity measurements should clarify the status of all these interesting objects.

6. Catalog of RR Lyr Stars

5455 RRab, 1655 RRc, 230 RRd and 272 RRe variable stars passed our selection criteria. Due to large number of objects the entire catalog is available only electronically from the OGLE INTERNET archive:

http://ogle.astrouw.edu.pl
ftp://ftp.astrouw.edu.pl/ogle/ogle2/var_stars/lmc/rrlyr/

or its US mirror

http://bulge.princeton.edu/˜ogle
ftp://bulge.princeton.edu/ogle/ogle2/var_stars/lmc/rrlyr/

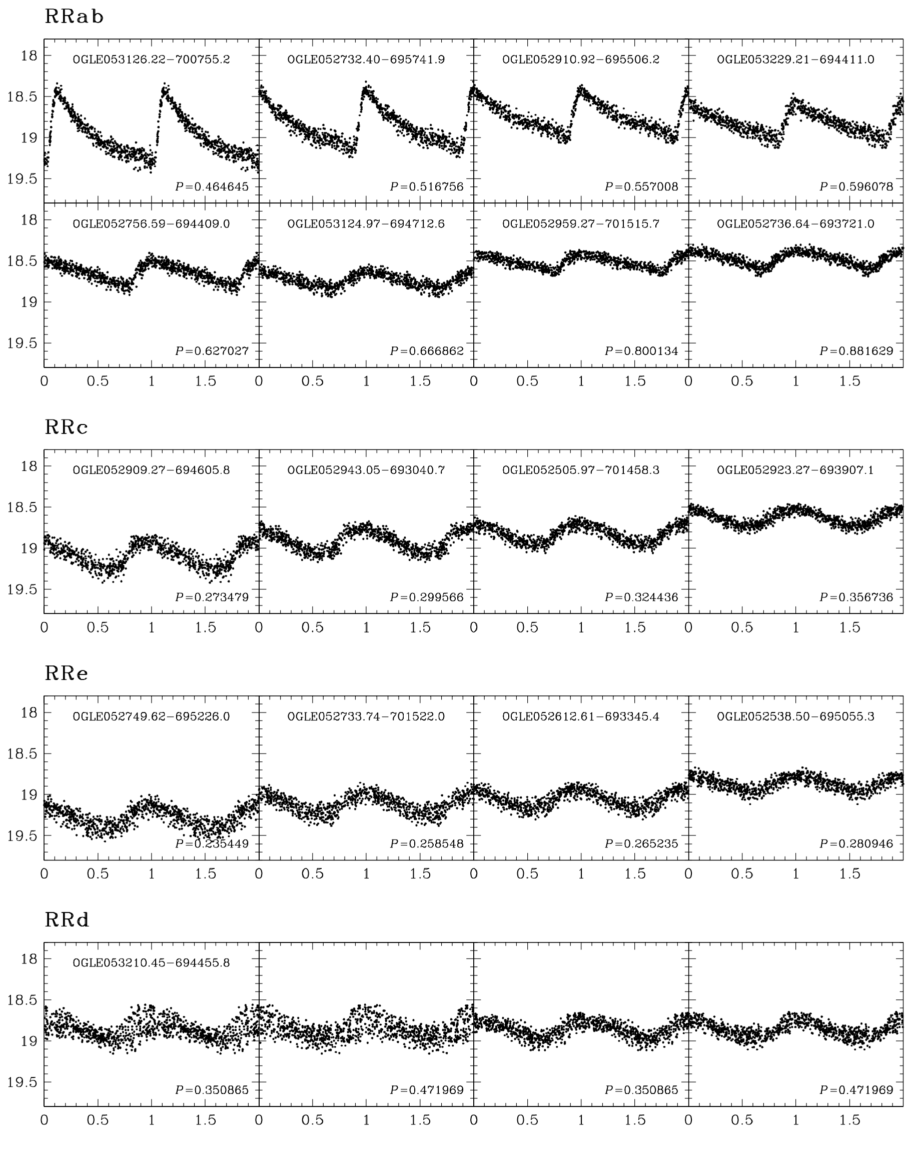

Fig. 3. Exemplary light curves of RR Lyr stars in the LMC. In the first two rows light curves of eight RRab stars arranged according to the periods are presented. In the next rows samples of RRc and RRe stars are presented. Bottom row shows the light curves of an exemplary RRd variable – original photometric data folded with the shorter and longer periods, and light curves of each mode after subtraction of the other period variability.

T a b l e 2

Exemplary single-mode RR Lyr stars from the LMC_SC1 field

Star ID	Star number	P [days]	$\sigma_{\rm P}$ [days]	T_0 -2450000	I [mag]	V [mag]	B [mag]	I_0 [mag]	V_0 [mag]	B_0 [mag]	A_I [mag]	A_V [mag]	A_B [mag]	R_{21}	ϕ_{21}	R_{31}	ϕ_{31}	Type
OGLE053232.25-703419.2	604	0.3419853	0.0000030	450.08450	18.77	19.22	–	18.54	18.84	–	0.28	0.38	–	–	–	–	–	c
OGLE053430.50-703411.3	184502	0.5428437	0.0000025	450.54199	18.57	19.14	19.45	18.34	18.76	18.94	0.61	0.82	1.18	0.49	4.26	0.36	2.36	ab
OGLE053312.35-703410.4	95386	0.6114353	0.0000032	450.24495	18.50	18.99	19.35	18.27	18.61	18.85	0.52	0.98	1.00	0.48	4.23	0.34	2.45	ab
OGLE053459.34-703404.9	267041	0.5128728	0.0000058	450.35384	18.55	19.67	–	18.32	19.29	–	0.65	1.58	–	0.47	4.03	0.41	1.97	ab
OGLE053334.45-703345.9	95453	0.5344097	0.0000015	450.53108	18.80	19.36	19.75	18.57	18.98	19.25	0.59	1.05	1.03	0.48	4.14	0.36	2.36	ab
OGLE053437.60-703338.0	267975	0.2965695	0.0000010	450.24258	18.87	19.25	19.45	18.64	18.87	18.95	0.38	0.47	0.63	0.21	4.56	0.08	3.51	c
OGLE053327.57-703332.3	95507	0.6095143	0.0000025	450.20909	18.64	19.07	–	18.41	18.70	–	0.37	0.54	–	0.43	4.59	0.26	3.17	ab
OGLE053423.87-703327.1	185332	0.3729185	0.0000006	450.24427	19.12	19.62	19.90	18.89	19.24	19.40	0.72	1.14	1.49	0.52	4.13	0.34	2.07	ab
OGLE053243.77-703244.5	888	0.6748426	0.0000089	450.06665	18.20	18.48	18.57	17.97	18.10	18.07	0.09	0.13	0.14	0.24	4.91	–	–	ab
OGLE053336.81-703241.2	95666	0.5783173	0.0000017	450.24576	18.75	19.36	19.71	18.52	18.98	19.20	0.52	0.83	1.01	0.45	4.38	0.36	2.68	ab
OGLE053458.97-703241.1	267359	0.5327837	0.0000010	450.47095	18.86	19.41	19.76	18.63	19.03	19.25	0.75	1.16	1.60	0.44	4.28	0.27	2.19	ab
OGLE053241.24-703240.3	910	0.5126785	0.0000008	450.50571	18.81	19.14	19.81	18.58	18.76	19.31	0.73	1.10	1.42	0.47	4.09	0.40	2.16	ab
OGLE053311.76-703230.4	97717	0.3891077	0.0000024	450.14003	19.36	19.62	19.81	19.13	19.25	19.31	0.34	0.49	0.65	0.20	5.78	–	–	c
OGLE053340.84-703228.3	95708	0.2796815	0.0000021	450.00456	18.81	19.20	19.39	18.58	18.83	18.89	0.14	0.29	0.38	0.20	4.84	–	–	c
OGLE053437.31-703225.3	268296	0.5670980	0.0000012	450.07732	18.64	19.19	19.46	18.41	18.81	18.95	0.57	0.87	0.99	0.49	4.28	0.35	2.41	ab
OGLE053354.20-703220.8	184794	0.6167336	0.0000025	450.52923	18.65	19.19	19.52	18.42	18.81	19.01	0.55	0.87	1.29	0.48	4.43	0.27	2.71	ab
OGLE053458.34-703213.6	268336	0.3457185	0.0000012	450.13368	18.87	19.37	19.81	18.64	18.99	19.30	0.34	0.53	0.78	0.22	4.79	0.11	3.69	c
OGLE053420.96-703211.7	185621	0.2692326	0.0000012	450.04477	19.00	19.36	19.54	18.77	18.98	19.03	0.21	0.34	0.40	0.20	4.56	–	–	c
OGLE053411.33-703151.2	185701	0.4775322	0.0000007	450.38008	18.81	19.29	–	18.58	18.91	–	0.86	1.36	–	0.47	4.03	0.34	1.93	ab
OGLE053403.50-703150.8	184376	0.6069833	0.0000020	450.29635	17.68	18.55	19.42	17.45	18.17	18.91	0.16	0.27	0.35	0.49	4.34	0.32	2.85	ab
OGLE053320.75-703133.4	95852	0.4817637	0.0000019	450.38633	18.98	19.43	19.87	18.75	19.06	19.36	0.70	1.11	1.60	0.40	4.05	0.20	1.88	ab
OGLE053427.31-703125.1	184985	0.5375598	0.0000011	450.41496	18.86	19.41	19.71	18.63	19.03	19.21	0.64	0.99	1.43	0.55	4.18	0.36	2.42	ab
OGLE053507.10-703113.3	268557	0.5729281	0.0000014	450.31329	18.72	19.27	19.67	18.50	18.90	19.17	0.68	1.09	1.58	0.50	4.37	0.30	2.47	ab
OGLE053418.64-703043.6	188173	0.5854574	0.0000013	450.24556	18.77	19.32	19.71	18.55	18.94	19.21	0.59	0.86	1.20	0.50	4.31	0.33	2.68	ab
OGLE053227.66-703032.6	4935	0.6473300	0.0000046	450.56484	18.88	19.49	19.88	18.65	19.11	19.38	0.25	0.42	0.57	0.46	4.57	0.22	3.40	ab
OGLE053240.80-703020.5	4977	0.6485066	0.0000051	450.57486	18.57	19.16	19.55	18.34	18.78	19.04	0.18	0.25	0.36	0.28	4.57	0.19	2.93	ab

In tables we provide the following data for each object: star ID (which includes equatorial coordinates of the star, RA and DEC, for the epoch 2000.0), star number (consistent with published LMC maps, Udalski *et al.* 2000), period in days, period error, moment of the zero phase corresponding to maximum light, intensity mean *IVB* photometry, extinction free magnitudes, amplitudes of the *IVB*-band light curves, Fourier parameters of the light curve decomposition and pulsation type. As an example we present in Table 2 the data for the first 27 single-mode RR Lyr variables.

Individual *BVI* observations of all objects and finding charts are also available from the OGLE INTERNET archive. For double-mode RR Lyr stars we provide both periods, period ratios, and other parameters, separately for fundamental mode and first-overtone of each star. Additionally, we provide the lists of multi-periodic RR Lyr stars probably pulsating in non-radial modes and objects found in star clusters in the LMC.

The lists contain altogether 8117 entries but only 7612 objects, because 500 RR Lyr stars were detected twice or even three times in the overlapping regions between adjacent fields. One of the files in the archive contains cross-reference list to identify stars in the overlapping regions.

Several exemplary light curves of all classes of RR Lyr stars are presented in Fig. 3. The light curves of RRab, RRc and RRe stars are arranged according to periods. One should note that the diagrams have the same magnitude range to compare the amplitudes and brightness of stars.

7. RR Lyr Stars in the LMC Star Clusters

Studies of RR Lyr stars in star clusters may provide significant clues to several problems in the theory of pulsation and stellar evolution. Traditionally, RR Lyr stars indicate a population of 11 or more Gyr old, although there is no strong evidence that can rule out their presence in substantially younger stellar systems. Therefore, detection of RR Lyr variables in star clusters younger than about 10 Gyr would have direct consequences on our ideas about evolution of old stellar systems. Discovery of RR Lyr stars in the substantial number of star clusters in the LMC may provide better understanding of the Oosterhoff dichotomy (Oosterhoff 1939).

We used the OGLE catalog of the LMC star clusters (Pietrzyński *et al.* 1999) containing 745 clusters, their coordinates and angular sizes, to select RR Lyr stars from the LMC clusters. We scanned our sample of RR Lyr variables looking for stars in a distance smaller than the cluster radius from the cluster center.

Since the cores of some star clusters are extremely dense, we put additional effort for detecting RR Lyr stars in those regions. For stars located near the center of the richest star clusters we lowered the limit for the signal-to-noise parameter of the light curve and then checked visually all new candidates. We improved in this way the completeness of our sample, but the completeness of our catalog is still the lowest in the cores of star clusters (see Section 9). We also stress that many stars in the central parts of the clusters are often severely blended.

In 6 clusters, namely NGC 1835, NGC 1898, NGC 1916, NGC 1928, NGC 2005, and NGC 2019, we found more than 6 RR Lyr stars. The results of our search are summarized in Table 3.

T a b l e 3

Star clusters containing RR Lyr stars

Cluster name	RA (J2000)	Dec (J2000)	Cluster radius [$''$]	N_{RR}	N_{ab}	N_c	N_e	N_d	N_{field} (estimated)
NGC1835	$5^h05^m07^s$	$-69°24'14''$	70	84	55	21	2	6	2
NGC1898	$5^h16^m41^s$	$-69°39'24''$	35	28	17	10	1	0	1
NGC1916	$5^h18^m38^s$	$-69°24'23''$	62	14	7	7	0	0	3
NGC1928	$5^h20^m58^s$	$-69°28'40''$	31	7	6	1	0	0	1
NGC2005	$5^h30^m10^s$	$-69°45'10''$	57	11	6	4	1	0	2
NGC2019	$5^h31^m56^s$	$-70°09'33''$	49	41	24	13	2	2	1

In all these cases it is extremely unlikely that all detected RR Lyr stars are simply field stars in the foreground or background of the clusters. To make sure that the majority of RR Lyr stars are the cluster members, we estimated the number of field RR Lyr variables, which should lie in the line-of-sight of the clusters. We counted RR Lyr stars from our sample in the ring around each cluster. The inner radius of the ring was set to $100''$ and the outer to $400''$. Comparing angular field of the ring and cluster, we derived the expected number of field RR Lyr stars inside the cluster area. These numbers are also provided in Table 3. They are significantly smaller than the number of detections.

In several clusters we found one, two or three RR Lyr stars. As the number of expected field RR Lyr stars is similar we are unable to conclude whether these stars are real members of clusters, or they are near the line-of-sight of the clusters by an optical coincidence.

NGC 1835 is the most compact star cluster in the observed region of the LMC. Graham and Ruiz (1974) and Walker (1992) surveyed this object for RR Lyr variables and discovered in total 36 such stars. We detected 84 RR Lyr variables: 55 RRab, 21 RRc, 6 RRd and 2 RRe stars. The period distribution of these stars is presented in Fig. 4. It is worth noticing that fundamental mode pulsators exhibit two peaks in the period histogram – near 0.54 and 0.65 days. These peaks correspond to the well-known mean periods of the Oosterhoff type I (OoI) and Oosterhoff type II (OoII) clusters (Smith 1995).

The second parameter which is used for distinction of the Oosterhoff's types is the ratio of the overtone RR Lyr stars to the total number of RR Lyr variables

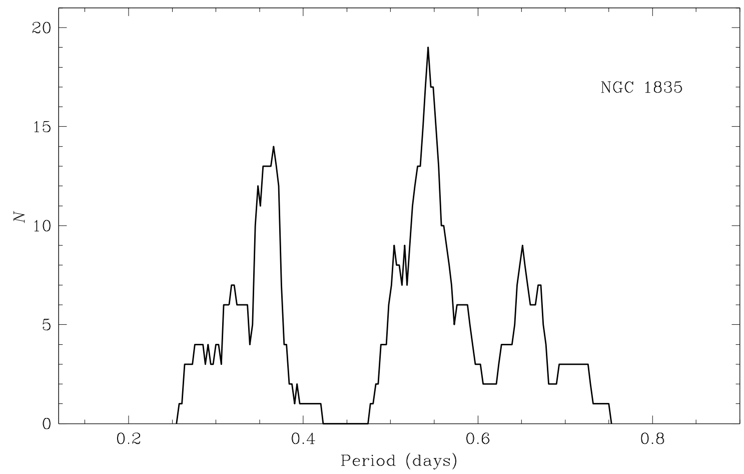

Fig. 4. Distribution of periods of 84 RR Lyr stars from the star cluster NGC 1835. The function was obtained from ten histograms (with 0.03 days wide bins), shifted by 0.003 days to each other.

($(N_c + N_d + N_e)/N_{RR}$). For NGC 1835 this parameter is equal to 0.34, *i.e.*, between the typical values for OoI (0.17) and OoII (0.44). We conclude that NGC 1835 shares the features of both Oosterhoff groups.

8. Basic Parameters of RR Lyr Stars

8.1. Period Distribution

The period histogram is a widely used tool for studying RR Lyr stars in galaxies and globular clusters because pulsational periods are unaffected neither by the distance nor by the interstellar reddening, and can be measured with the highest precision. Comparative analysis of the distributions of RR Lyr variables from various stellar systems yields information about the early history of star formation.

The distribution of periods of 7612 RR Lyr stars is presented in Fig. 5. The function is composed of series of ten histograms (bin width 0.01 days) shifted by 0.001 days with respect to each other. This manner of the period distribution presentation enables precise determination of the most likely periods of all types of the RR Lyr stars.

The mean period of ab-type RR Lyr stars is $\langle P_{ab} \rangle = 0.573$ days. This is a slightly lower value than that found by the MACHO team: $\langle P_{ab} \rangle = 0.583$ days (Alcock *et al.* 1996). The most likely period of RRc variables is equal to $\langle P_c \rangle = 0.339$ days, what agrees well with the value obtained by MACHO (0.342 days).

Alcock *et al.* (1996) also detected a secondary peak in the period distribution of the overtone pulsators. They interpreted it as due to presence of the second overtone RR Lyr stars (RRe). Another explanation of the peak at $P = 0.281$ days was presented by Bono *et al.* (1997), who suggested that it could be a signature of a more metal-rich population of RR Lyr stars. Similar secondary peaks were

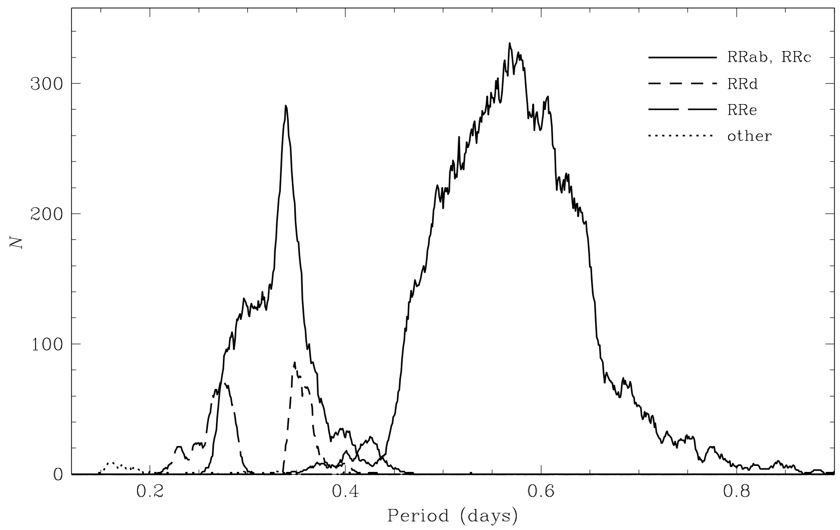

Fig. 5. Distribution of periods for RR Lyr stars in the LMC. The function was obtained from ten histograms (with 0.01 days wide bins), shifted by 0.001 days to each other. Solid lines correspond to RRab and RRc stars, short-dashed line represents the first-overtone periods of RRd stars, long-dashed line – RRe stars, and dotted line – other stars.

also detected in the Sculptor dwarf spheroidal galaxy (Kałużny *et al.* 1995), in the Oosterhoff type I and type II Galactic globular clusters (Clement *et al.* 2001) and in the Small Magellanic Cloud (Paper I).

The secondary peak disappears when we separated first- and second-overtone RR Lyr stars. In Fig. 5 the period distribution of objects classified by us as RRe stars is presented separately. The most likely period of these pulsators is $\langle P_e \rangle = 0.276$ days, giving the mean $P_e/P_c = 0.814$.

In Fig. 5 we also present the distribution of the first-overtone period of double-mode RR Lyr stars. The function has a sharp maximum at $P_d = 0.348$ days.

8.2. Period-Luminosity Relations and Mean Magnitude

Similarly to Paper I we derived the *BVI* intensity mean photometry for each object from our catalog. The light curves converted to the intensity units were approximated by the Fourier series of fifth order and integrated. Results were converted back to the magnitude scale. Accuracy of the mean *I*-band photometry is about 0.02 mag while that of the *V*-band and *B*-band about 0.05 mag and 0.08 mag, respectively, what is a consequence of smaller number of observations in the *BV*-bands.

For each star we also determined the reddening free Wesenheit index (Madore 1982), defined as:

$$W_I = I - 1.55(V - I)$$

where 1.55 is the ratio of total-to-selective absorption $(A_I/E(V-I))$.

Figs. 6 and 7 show the period–magnitude and period–W_I diagrams, respec-

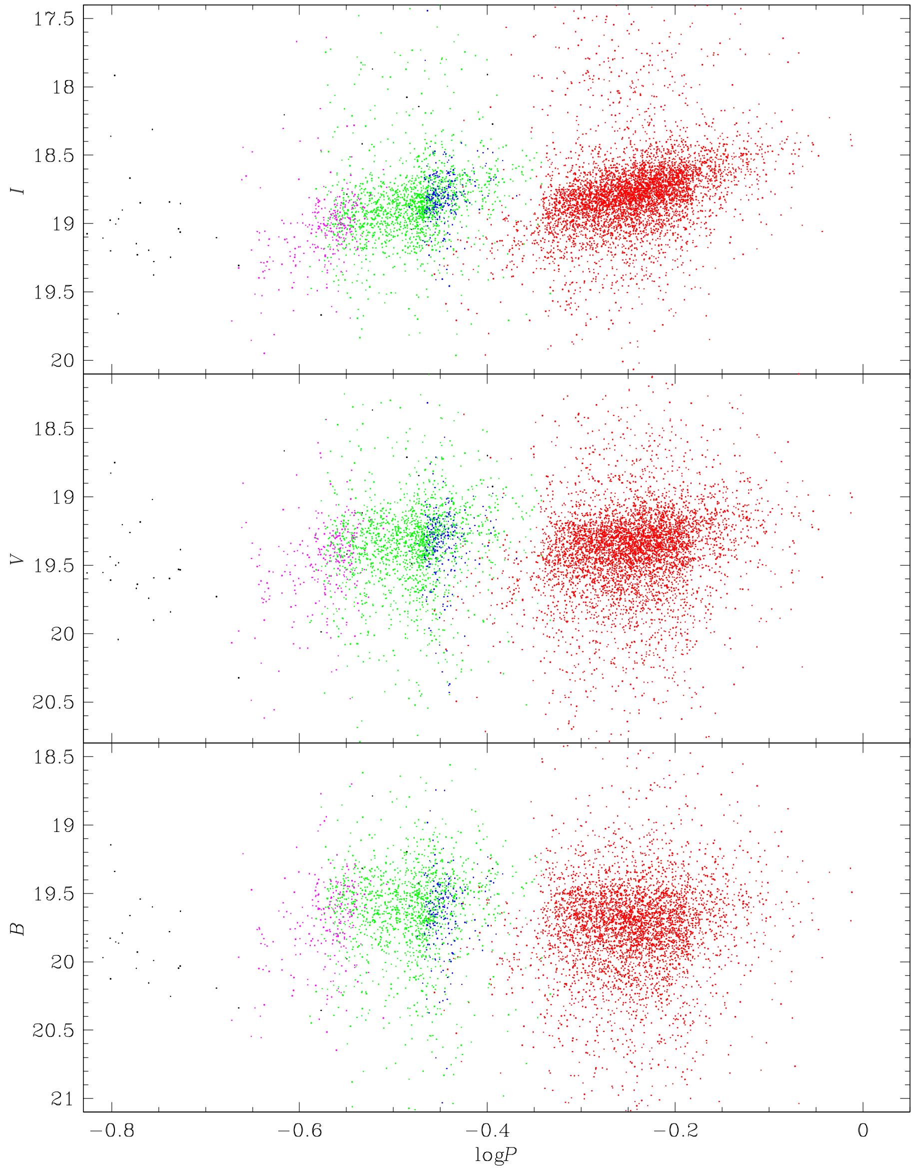

Fig. 6. *IVB*-band period–luminosity diagrams for RR Lyr stars in the LMC. Red points represent RRab stars, green – RRc, blue – RRd (first-overtone), magenta – RRe, and black points – other stars.

tively. One can notice that many stars are significantly brighter than typical RR Lyr variables from the LMC while some are fainter. We left these stars on our list because they reveal all characteristics of the RR Lyr-type light curves. Since the LMC fields are very crowded it is very likely that many of these variables are blended with other stars. Although quality of DIA photometry is much better compared to the standard profile photometry, it is impossible to separate blended stars, because the non-variable component of the photometry is measured with traditional

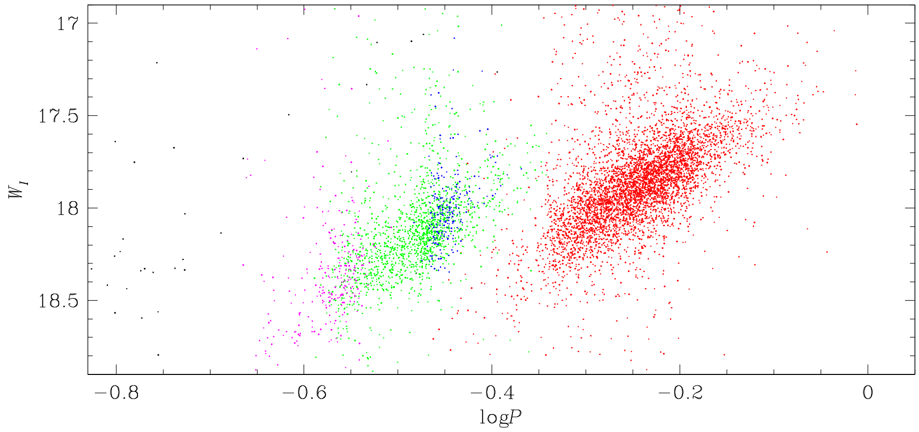

Fig. 7. Period–luminosity diagram for extinction insensitive index $W_I = I - 1.55(V - I)$. Color of points represent the same RR Lyr types as in Fig. 6.

methods in the reference image. In some cases, in particular when a measured star is located very close to other bright star, it is impossible to determine correct magnitudes.

Moreover, other types of variable stars, *e.g.*, δ Sct and Anomalous Cepheids with similar light curves to RR Lyr stars might be included to our catalog. They can be brighter or fainter than typical RR Lyr star. Finally, there are RR Lyr stars which are located in the halo of the LMC, thus, in front or behind the central parts of the galaxy, *i.e.*, brighter or fainter, respectively.

Nevertheless, most of the RR Lyr stars form distinct sequences in the period–luminosity diagrams. To derive period–luminosity relations we performed the following procedure for RRab and RRc stars, separately. First, we prepared histograms of the *BVI*-band magnitudes and W_I index at several discrete values of $\log P$ (0.03 wide bins in $\log P$). In the next step we fitted a Gaussian to each of the histograms and determined maximum of the function, *i.e.*, we obtained the most likely brightness for a given period. Finally, we fitted a linear function to the $\log P$–magnitude points.

We obtained strong period–luminosity relation for the *I*-band and rather weak correlation of $\log P$ and *V*-band mean magnitudes for both, ab-type and c-type RR Lyr stars. We did not detect any statistically significant $\log P - B$ relation. Therefore we derived the most likely magnitude of the RR Lyr stars in the *B*-band by fitting a Gaussian to the histograms prepared for the whole sample of RR Lyr stars of a given type.

The period–luminosity relations for RRab stars in the LMC are as follows:

$$
\begin{aligned}
I &= -1.62(\pm 0.05)\log P + 18.391(\pm 0.011)\\
V &= -0.80(\pm 0.08)\log P + 19.150(\pm 0.014)\\
B &= 19.71(\pm 0.03)\\
W_I &= -2.75(\pm 0.04)\log P + 17.217(\pm 0.008)
\end{aligned}
$$

for RRc stars:

$$
\begin{aligned}
I &= -2.23(\pm 0.03)\log P + 17.840(\pm 0.007)\\
V &= -1.03(\pm 0.08)\log P + 18.807(\pm 0.012)\\
B &= 19.58(\pm 0.02)\\
W_I &= -2.88(\pm 0.06)\log P + 16.787(\pm 0.015)
\end{aligned}
$$

Because the sample of RRe candidates is less numerous, we derived the period–luminosity relations by fitting a linear function to the mean magnitudes:

$$
\begin{aligned}
I &= -3.24(\pm 0.20)\log P + 17.182(\pm 0.012)\\
V &= -2.24(\pm 0.20)\log P + 18.156(\pm 0.015)\\
B &= 19.68(\pm 0.04)\\
W_I &= -4.02(\pm 0.08)\log P + 16.337(\pm 0.011)
\end{aligned}
$$

It is worth noticing that generally the slope of the period–luminosity relation depends on the type of RR Lyr object. The dependence is steeper for stars pulsating in higher modes.

Kovács and Walker (2001) derived period–luminosity–color relations for a sample of RR Lyr stars of ab type from the Galactic globular clusters. They determined the dependence of period and quantity defined as $X = V - 2.5(V - I)$, where I and V are magnitude average photometry. For comparison we calculated magnitude average luminosities for our sample of RRab stars and found $\log P$–X relation. The slope obtained by Kovács and Walker (2001), -2.51 ± 0.07, is in very good agreement with our value: -2.55 ± 0.05.

RR Lyr stars are widely accepted as very good distance indicator and their mean magnitude in the V-band is often used for distance determinations. As we show in Fig. 6 the V-band magnitude might be somewhat dependent on the pulsation period, but the correlation is relatively weak in that band. Therefore we may determine the mean magnitudes of these stars in the LMC for future precise determination of the distance to this galaxy. The modal value of the distribution of the observed V-band magnitude of our sample of RR Lyr is equal to 19.36 ± 0.03 mag and 19.31 ± 0.02 mag for ab and c types, respectively. For magnitudes dereddened with the OGLE-II reddening map (Section 3) the appropriate values are: 18.91 ± 0.02 and 18.89 ± 0.02, again for ab and c types, respectively.

8.3. Period-Amplitude Relations

The period–amplitude diagram, known as Bailey diagram, is a widely used tool for analyzing features of RR Lyr stars. Empirical and theoretical studies suggest that the distribution of RR Lyr stars in the Bailey diagram depends on their metallicity. In Fig. 8 we plot the period–amplitude diagram for RR Lyr stars from our catalog.

Fundamental mode RR Lyr stars present an anti-correlation between the period and amplitude. Due to large number of RRab stars one can notice that the sequence

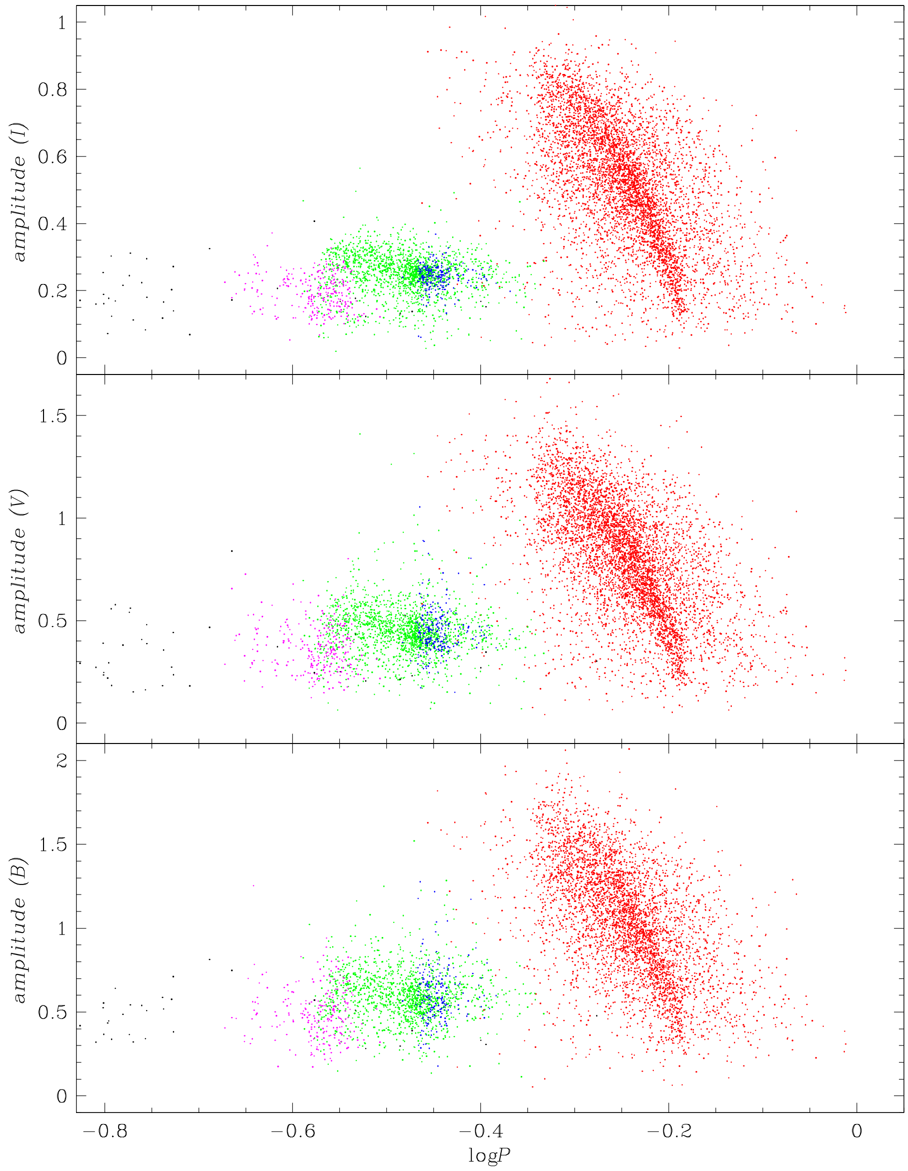

Fig. 8. *IVB*-band period–amplitude diagrams for RR Lyr stars in the LMC. Color of points represent the same RR Lyr types as in Fig. 6.

in the $\log P$–amplitude diagram is non-linear, what agrees with theoretical models (Bono *et al.* 1997). The width of the sequence is believed to be an effect of spread in the metal content.

Distribution of the overtone pulsators in the Bailey diagram is more complicated. RRc and RRe stars present a weak anti-correlation of amplitudes and periods, and form continuous but overlapping sequences. The period–amplitude plot was an auxiliary tool to the $\log P$–R_{21} diagram that was used for separation of the first-and second-overtone RR Lyr stars.

8.4. Fourier Coefficients

The *I*-band light curves of our RR Lyr candidates were fitted to the Fourier series of the fifth order. Then, the Fourier parameters R_{21}, R_{31}, ϕ_{21} and ϕ_{31} were derived, where $R_{ij} = A_i/A_j$, $\phi_{ij} = \phi_i - i\phi_j$. A_i and ϕ_i are the amplitude and phase terms of $(i-1)$ harmonic of the Fourier decomposition of light curve.

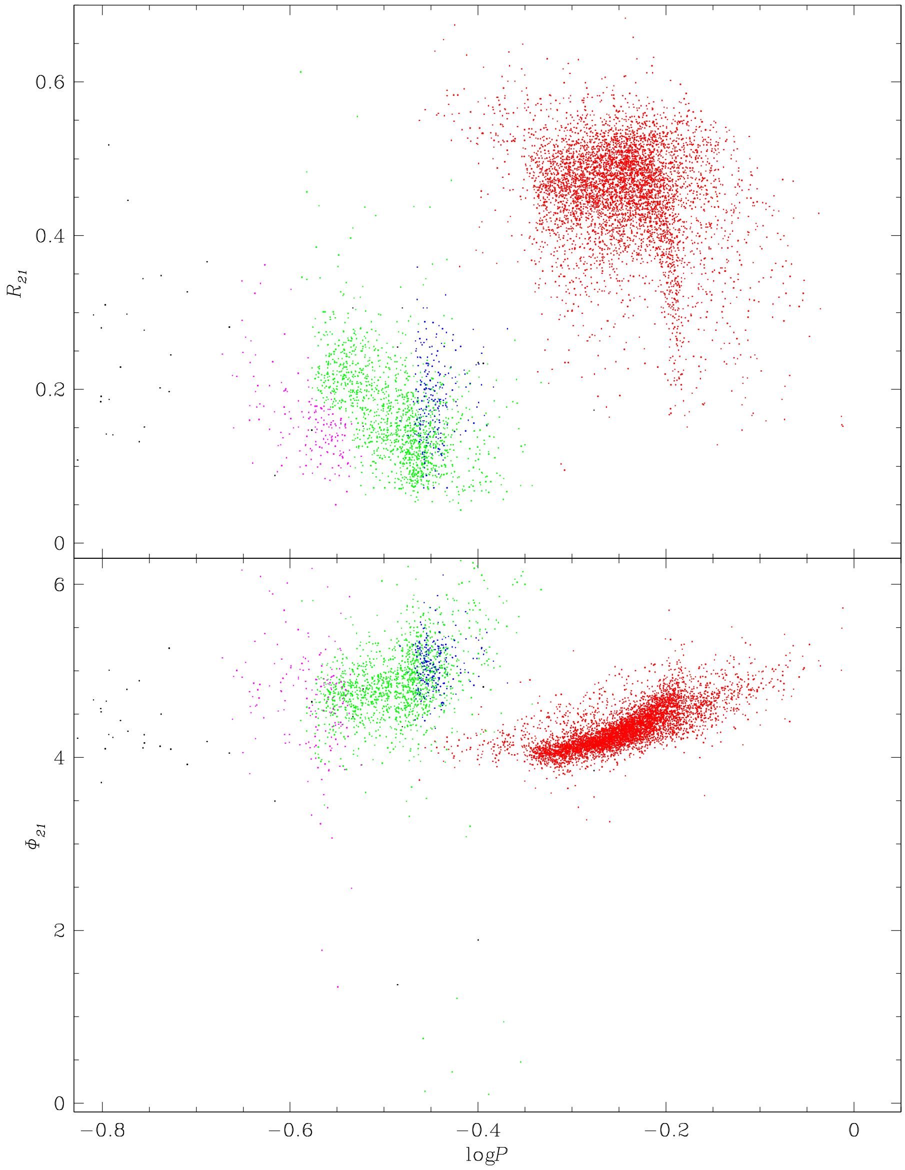

Fig. 9. R_{21} and ϕ_{21} *vs.* $\log P$ diagrams for RR Lyr stars in the LMC. Color of points represent the same RR Lyr types as in Fig. 6.

The R_{ij} and ϕ_{ij} parameters are widely used for analyzing properties of the light curves of pulsating stars. Using empirical and theoretical relations it is possible to derive physical characteristics of RR Lyr stars, including mass, absolute magnitude, effective temperature and metallicity (*e.g.*, Kovács and Walker 2001).

In Fig. 9 we plot $\log P$–R_{21} and $\log P$–ϕ_{21} diagrams constructed for our sample of RR Lyr stars. $\log P$–R_{21} diagram is particularly useful for dividing single-mode RR Lyr stars into three classes: RRab, RRc and RRe, because these groups occupy different regions in the diagram. The R_{21} parameter for each class of single-mode RR Lyr variables tends to become smaller as the periods become longer. On the other hand the ϕ_{21} parameter of the RRab, RRc and RRe stars increases with periods. That means that the light curves of RR Lyr with longer periods are more sinusoidal and more symmetrical than the light curves of stars with shorter periods pulsating in the same mode.

Light curves of the first-overtone mode of double-mode pulsators seem to be on average more "sharp" than those of single mode stars with corresponding periods (*i.e.*, between 0.46 and 0.58 days). The fundamental mode pulsation of RRd stars has R_{21} smaller than corresponding single-mode RR Lyr variables, what means that the light curves are more sinusoidal than the light curves of RRab stars.

8.5. Petersen Diagram

The period *vs.* period ratio diagram for double-mode pulsators, the so called Petersen diagram (Petersen 1973), is a powerful tool providing substantial information about the mass and metallicity of pulsating stars (Popielski, Dziembowski and Cassisi 2000). Since periods are firm and accurate observables, P_0 *vs.* P_1/P_0 diagram together with theoretical models of double-mode RR Lyr stars makes it possible to study various problems, including, for instance, the LMC distance scale (Kovács 2000).

In Fig. 10 we show the Petersen diagram for 230 RRd stars from the LMC. Compared to double-mode RR Lyr stars from the Galactic globular clusters and also from other galaxies of the Local Group, RRd variables in the LMC cover wide range of periods and period ratios, although most of stars concentrate near the shortest periods of the sequence. As concluded by Popielski, Dziembowski and Cassisi (2000) such a wide spread of periods probably indicates wide spread of metal content.

9. Completeness of the Catalog

The probability that a given RR Lyr star has been included to our catalog depends on several factors like its amplitude, luminosity and crowding in its vicinity. The completeness of the catalog was estimated in similar way as the completeness of the catalog of RR Lyr stars in the Small Magellanic Cloud (Paper I), *i.e.*, by comparison of objects detected in the overlapping regions between the neighboring fields. Twenty three such regions exist between our fields, allowing to perform 46 tests of paring objects from a given and adjacent fields. In total, 1079 stars from

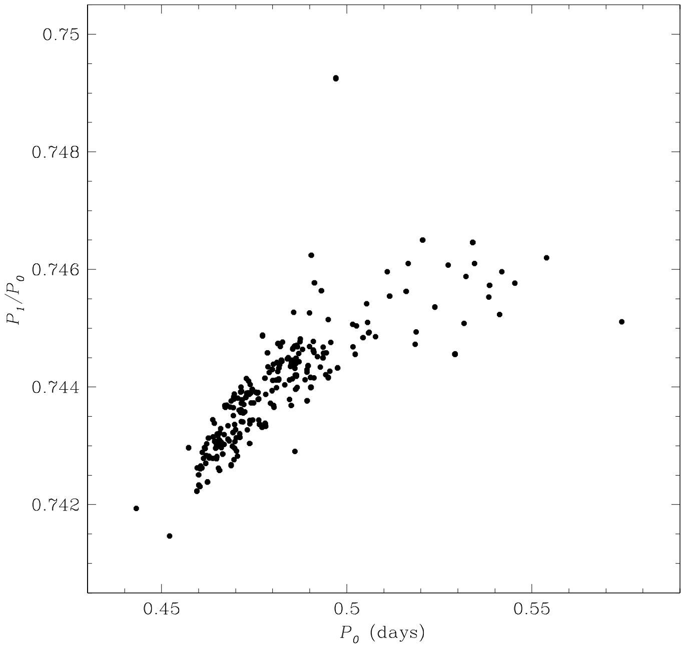

Fig. 10. Petersen diagram for the LMC RRd stars.

our lists should be paired with counterparts in the overlapping fields. We found counterparts in 1022 cases, which yields the completeness of our full sample equal to about 95%.

One should, however, remember that there is a number of variables which were missed in both overlapping fields. The regions near the edges of the fields are biased by smaller number of measurements, due to imperfections in the telescope pointing, what reduces the completeness of the catalog in the edge regions. We checked carefully all instances of unpaired objects. Counterparts of ten unpaired objects have the number of observations smaller than 100 and thus they were not searched for variability. More than 20 missed stars are located in the cores of dense star clusters or were blended with a bright star. That means that the completeness of the RR Lyr sample detected in the star clusters is much lower than for the remaining regions. It is also possible that some RR Lyr stars located close to the line-of-sight of bright stars could be missed.

Additionally, we compared our sample to the MACHO list of 8654 RR Lyr stars from the LMC, retrived from the MACHO archive

(*http://wwwmacho.mcmaster.ca/Data/MachoData.html*).

3257 stars from the MACHO list could potentially be found in our fields. We did not find counterparts for 74 objects. Most of the missed stars were not RR Lyr stars. The real RR Lyr stars that were not identified in our sample were usually located very close to the edge of the frame and therefore they were biased by small number of observations.

10. Summary

In this paper we presented a huge sample of 7612 RR Lyr stars found in the OGLE-II fields in the LMC. The mean parameters of all stars and individual measurements spanning four years of OGLE-II phase of the project are now available to the astronomical community. This is an ideal and unique dataset for further extensive studies of RR Lyr stars.

The third phase of the OGLE project (OGLE-III) started in June 2001 (Udalski *et al.* 2002) after significant increase of the observing capability. With the new mosaic CCD camera with the field of view increased to $35' \times 35'.5$ and sampling 0.25 arcsec/pixel almost entire Magellanic Clouds are now regularly monitored. Therefore, in the time scale of a few years complete catalogs of the vast majority of variable stars from both Magellanic Clouds should be released by the OGLE project.

Acknowledgements. We are grateful to Prof. B. Paczyński for constant support and many useful suggestions during preparation of this paper. We thank Prof. W. Dziembowski for discussions and many important remarks. Also, we would like to thank Mr. Z. Kołaczkowski for help in estimation of the catalog completeness and providing the FNPEAKS software. We are very grateful to Prof. G. Kovács for valuable comments to this work. The paper was partly supported by the Polish KBN grant 2P03D02124 to A. Udalski. Partial support to the OGLE project was provided with the NSF grant AST-0204908 and NASA grant NAG5-12212 to B. Paczyński.

This paper utilizes public domain data originally obtained by the MACHO Project, whose work was performed under the joint auspices of the U.S. Department of Energy, National Security Administration by the University of California, Lawrence Livermore National Laboratory under contract No. W-7405-Eng-48, the National Science Foundation through the Center for Particle Astrophysics of the University of California under cooperative agreement AST-8809616, and the Mount Stromlo and Siding Spring Observatory, part of the Australian National University.

REFERENCES

Alard, C., and Lupton, R.H. 1998, *Astrophys. J.*, **503**, 325.
Alard, C. 2000, *Astron. Astrophys. Suppl. Ser.*, **144**, 363.
Alcock, C., *et al.* (MACHO team) 1996, *Astron. J.*, **111**, 1146.
Alcock, C., *et al.* (MACHO team) 1997, *Astrophys. J.*, **482**, 89.
Alcock, C., *et al.* (MACHO team) 2000, *Astrophys. J.*, **542**, 257.
Bono, G., Caputo, F., Cassisi, S., Incerpi, R., and Marconi, M. 1997, *Astrophys. J.*, **483**, 811.
Clement, C., and Rowe, J. 2000, *Astron. J.*, **120**, 2579.
Clement, C., *et al.* 2001, *Astron. J.*, **122**, 2587.
Clementini, G., Gratton, R., Bragaglia, A., Carretta, E., Di Fabrizio, L., and Maio, M. 2003, *Astron. J.*, **125**, 1309.
Dziembowski, W., and Cassisi, S. 1999, *Acta Astron.*, **49**, 371.

Graham, J.A., and Ruiz, M.T. 1974, *Astron. J.*, **79**, 363.
Graham, J.A. 1977, *P.A.S.P.*, **89**, 425.
Hazen, M.L., and Nemec, J.M. 1992, *Astron. J.*, **104**, 111.
Kałużny, J., Kubiak, M., Szymański, M., Udalski, A., Krzemiński, W., and Mateo, M. 1995, *Astron. Astrophys. Suppl. Ser.*, **112**, 407.
Kinman, T.D., Stryker, L.L., and Hesser, J.E. 1976, *P.A.S.P.*, **88**, 393.
Kovács, G. 1998, "A Half-Century of Stellar Pulsation Interpretations", Ed. P.A. Bradley and J.A. Guzik, *ASP Conference Series*, Vol. **135**, 53.
Kovács, G. 2000, *Astron. Astrophys.*, **363**, L1.
Kovács, G., and Walker, A.R. 2001, *Astron. Astrophys.*, **371**, 579.
Madore B.F. 1982, *Astrophys. J.*, **253**, 575.
Moskalik, P. 2000, in: *IAU Colloq.* 176, "The Impact of Large-Scale Surveys on Pulsating Star Research", Ed. L. Szabados and D.W. Kurtz, *ASP Conference Series*, Vol. **203**, 135.
Nemec, J.M., Hesser, J.E., and Ugarte, P. 1985, *Astrophys. J. Suppl. Ser.*, **57**, 287.
Nowakowski, R.M., Dziembowski, W.A. 2001, *Acta Astron.*, **51**, 5.
Olech, A., *et al.* 1999, *Astron. J.*, **118**, 442.
Oosterhoff, P.Th. 1939, *The Observatory*, **62**, 104.
Petersen, J.O. 1973, *Astron. Astrophys.*, **27**, 89.
Pietrzyński, G., Udalski, A., Kubiak, M., Szymański, M., Woźniak, P., and Żebruń, K. 1999, *Acta Astron.*, **49**, 521.
Popielski, B.L., Dziembowski, W.A., and Cassisi, S. 2000, *Acta Astron.*, **50**, 491.
Schechter, P.L., Saha, K., and Mateo, M. 1993, *P.A.S.P.*, **105**, 1342.
Schlegel, D.J., Finkbeiner, D.P., and Davis, M. 1998, *Astrophys. J.*, **500**, 525.
Schwarzenberg-Czerny, A. 1989, *MNRAS*, **241**, 153.
Soszyński, I., Udalski, A., Szymański, M., Kubiak, M., Pietrzyński, G., Woźniak, P., Żebruń, K., Szewczyk, O., and Wyrzykowski, Ł. 2002, *Acta Astron.*, **52**, 369 (Paper I).
Smith, H.A. 1995, RR Lyr Stars, (Cambridge University Press).
Stellingwerf, R.F., Gautschy, A., and Dickens, R.J. 1987, *Astrophys. J.*, **313**, L75.
Thackeray, A.D., and Wesselink, A.J. 1953, *Nature*, **171**, 693.
Udalski, A., Kubiak, M., and Szymański, M. 1997, *Acta Astron.*, **47**, 319.
Udalski, A., Szymański, M., Kubiak, M., Pietrzyński, G., Woźniak, P., and Żebruń, K. 1998a, *Acta Astron.*, **48**, 147.
Udalski, A., Soszyński, I., Szymański, M., Kubiak, M., Pietrzyński, G., Woźniak, P., and Żebruń, K. 1998b, *Acta Astron.*, **48**, 563.
Udalski, A., Soszyński, I., Szymański, M., Kubiak, M., Pietrzyński, G., Woźniak, P., and Żebruń, K. 1999a, *Acta Astron.*, **49**, 223.
Udalski, A., Soszyński, I., Szymański, M., Kubiak, M., Pietrzyński, G., Woźniak, P., and Żebruń, K. 1999b, *Acta Astron.*, **49**, 437.
Udalski, A., Szymański, M., Kubiak, M., Pietrzyński, G., Soszyński, I., Woźniak, P., and Żebruń, K. 2000, *Acta Astron.*, **50**, 307.
Udalski, A., Paczyński, B., Żebruń, K., Szymański, M., Kubiak, M., Soszyński, I., Szewczyk, O., Wyrzykowski, Ł., and Pietrzyński, G. 2002, *Acta Astron.*, **52**, 1.
Van Hoolst, T., Dziembowski, W.A., and Kawaler, S.D. 1998, *MNRAS*, **297**, 536.
Walker, A.R. 1992, *Astrophys. J.*, **390**, L81.
Woźniak, P. R. 2000, *Acta Astron.*, **50**, 421.
Wyrzykowski, Ł., Udalski, A., Kubiak, M., Szymański, M., Żebruń, K., Soszyński, I., Woźniak, P., Pietrzyński, G., and Szewczyk, O. 2003, *Acta Astron.*, **53**, 1.
Żebruń, K., Soszyński, I., and Woźniak, P.R. 2001, *Acta Astron.*, **51**, 303.
Żebruń, K., Soszyński, I., Woźniak, P., Udalski, A., Kubiak, M., Szymański, M., Pietrzyński, G., Szewczyk, O., and Wyrzykowski, Ł. 2001, *Acta Astron.*, **51**, 317.